Dynamics of kinematically constrained bimolecular reactions having constant product recoil energy

Cite as: J. Chem. Phys. **86**, 3968 (1987); https://doi.org/10.1063/1.451907
Submitted: 06 October 1986 . Accepted: 02 December 1986 . Published Online: 31 August 1998

Chifuru Noda, and Richard N. Zare

Dynamics of kinematically constrained bimolecular reactions having constant product recoil energy

Chifuru Noda and Richard N. Zare
Department of Chemistry, Stanford University, Stanford, California 94305

(Received 6 October 1986; accepted 2 December 1986)

A model is presented for kinematically constrained reactions in which the product recoil energy is assumed constant (CPR approximation). It is further assumed that the reaction probability is independent of both the impact parameter and the collision energy for all collisions that lead to products. This model predicts that (1) the product vibrational distribution is bell-shaped, peaking at the vibrational level with an energy equal to the reaction exoergicity minus the product recoil energy, (2) small values of the impact parameters produce high vibrational excitation while large values produced low vibrational excitation, the specific opacity function for the most populated vibrational level being sharply peaked at the impact parameter equal to the equilibrium internuclear distance of the product diatomic, (3) the product rotational distribution for each vibrational level differs but has the form of a sharp leading edge for some J value followed by a falloff whose shape depends on the form of the collision energy distribution, and (4) the product average rotational energy associated with each vibrational level decreases linearly with increasing v to a value of v corresponding to the maximum in the vibrational distribution followed by a more slowly changing behavior. Comparisons are made of these predictions with some experiments on kinematically constrained bimolecular reactions. Some further extensions of the CPR model are suggested.

I. INTRODUCTION

In a reactive encounter of a heavy atom A, and a heavy–light diatomic molecule BC to produce a heavy–heavy diatomic molecule AB plus a light atom C,

$$A + BC \rightarrow AB + C, \tag{1}$$

conservation of total angular momentum constrains the oribtal angular momentum of the reagents $|\mathbf{L}| = \mu b v_{\mathrm{rel}}$, to appear as rotational angular momentum $|\mathbf{J}|$ of the AB product.[1] Here μ is the reduced mass of the A–BC pair, b is called the impact parameter, which is defined as the distance of closest approach for undeflected trajectories, and v_{rel} is the relative velocity of the collision pair. This kinematic constraint allows experimentalists in principle to determine the impact parameter distribution for the reaction channel leading to a specific vibrational level, called the specific opacity function, from the product rotational distribution, provided that the relative velocity distribution of the collision partner leading to reaction is known.

We have developed a model which can be used to calculate the product vibrational distributions, the specific opacity functions, and the rotational distributions in each product vibrational level. The model is based on an assumption that the product recoil energy is a constant whose value does not depend on the collision energy and the impact parameter. We refer to this as the constant product recoil (CPR) model.

In general the product recoil energy is characterized by a distribution whose form varies with the product internal state distributions. However, for the kinematically constrained A + BC→AB + C reaction, it may be argued that the light leaving atom C moves so rapidly compared to the heavy–heavy AB pair that under some circumstances the same critical configuration is reached for any impact parameter and any (near thermal) collision energy. This suggests the CPR model might be an appealing first approximation. Further support for this model is provided for those kinematically constrained reactions which are described by an electron jump mechanism. In such cases, the DIPR-DIP (direct interaction product repulsion-dissociation as in photodissociation) model predicts a constant average recoil energy.[2] Siegel and Schultz carried out trajectory calculations on several model potential surfaces for kinematically constrained reactions.[3] They found that the product recoil energy is indeed a constant for the LEPS potential surfaces, although this is not a case for the HMF (hyperbolic map function) potential surfaces. These considerations have led us to investigate the consequences of this simple model.

II. THEORY

Consider the energy balance for the kinematically constrained reaction (1). We write for the energy of the reactants

$$E^i = E(A) + E(BC) - D(BC) + T^i \tag{2a}$$

and the energy of the products

$$E^f = E(AB) + E(C) - D(AB) + T^f, \tag{2b}$$

where i and f are the initial and final states, E refers to the internal energy, D the dissociation energy measured from the $v = 0$ vibrational level, and T the translational energy. For the AB product

 0021-9606/87/073968-10$02.10

$$E(\mathrm{AB}) = E_{\mathrm{vib}} + E_{\mathrm{rot}} , \tag{3}$$

where approximately

$$E_{\mathrm{vib}} \approx \omega_e v \tag{4a}$$

and

$$E_{\mathrm{rot}} \approx BJ^2 \approx \frac{J^2}{2\mu' r_e^2} . \tag{4b}$$

In Eq. (4b), μ' is the reduced mass and r_e is the equilibrium internuclear distance of the AB diatomic product. Due to the kinematic contraint,

$$|\mathbf{J}| = |\mathbf{L}| = \mu b v_{\mathrm{rel}} . \tag{5}$$

When C is light compared to A and B, $\mu' \approx \mu$. Since $T^i = (1/2)\mu v_{\mathrm{rel}}^2$, the AB rotational energy can be expressed as

$$E_{\mathrm{rot}} = (b/r_e)^2 T^i . \tag{6}$$

By equating E^i to E^f and by replacing E_{rot} by Eq. (6), we obtain the following expression for the AB vibrational energy:

$$E_{\mathrm{vib}} = [1 - (b/r_e)^2] T^i + \Delta E - T^f + E(\mathrm{A}) + E(\mathrm{BC}) - E(\mathrm{C}) , \tag{7}$$

where

$$\Delta E = D(\mathrm{AB}) - D(\mathrm{BC}) . \tag{8}$$

By invoking the CPR approximation we replace $\Delta E - T^f + E(\mathrm{A}) + E(\mathrm{BC}) - E(\mathrm{C})$ by a constant which we denote by A. Note that for the reaction in which the reagent atom A is in the ground state and the reagent molecule BC is cooled in supersonic expansion, we obtain $E(\mathrm{A}) = 0$ and $E(\mathrm{BC}) = 0$. Also if the product atom C is in the ground state, $E(\mathrm{C}) = 0$, and the expression for A reduces to $\mathrm{A} = \Delta E - T^f$, which is the difference between the exoergicity and the product recoil energy. After the substitution, Eq. (7) becomes

$$E_{\mathrm{vib}} = [1 - (b/r_e)^2] T^i + A . \tag{9}$$

Hence, for kinematically contrained reactions, the product vibrational energy becomes a function of the impact parameter and the relative initial kinetic energy. In other words, the (b/v_{rel}) pair maps *uniquely* onto the (v, J) state of the diatomic product.[4] For the case of constant product recoil energy, this relationship is remarkably simple.

We find it convenient to work with dimensionless reduced quantities, and take r_e as the unit of distance and ω_e as the unit of energy. Then Eq. (9) may be expressed as

$$v^* = [1 - b^{*2}] E^* + A^* . \tag{10}$$

Here

$$v^* = E_{\mathrm{vib}}/\omega_e \tag{11a}$$

is the product vibrational energy (as well as its vibrational quantum number),

$$E^* = T^i/\omega_e \tag{11b}$$

is the collision energy of the A–BC pair,

$$A^* = A/\omega_e , \quad = [\Delta E - T^f + E(\mathrm{A}) + E(\mathrm{BC}) - E(\mathrm{C})]/\omega_e \tag{11c}$$

is a constant expressing primarily the difference between the reaction exoergicity and the product recoil energy, and

$$b^* = b/r_e \tag{11d}$$

is the reduced impact parameter. We also introduce a quantity R^* to represent the product rotational energy:

$$R^* = b^{*2} E^* . \tag{12}$$

The vibrational and rotational energies are treated differently as follows; if the vibrational energy is between $v^* - 1/2$ and $v^* + 1/2$, the vibrational level v^* is considered to be populated, and the width of the vibrational state is one energy unit. The rotational state has a range of the rotational energy between $R^* - dR^*/2$ and $R^* + dR^*/2$ and a width given by the infinitesimal dR^*.

Figure 1 shows "phase space" of b^* and E^* for different product vibrational states with A^* set to 10 as an example. Into which band the (b^*, E^*) pair falls determines the product vibrational energy. Figure 2 depicts the rotational energy contour of the (b^*, E^*) pair in phase space. Note that the phase space bands cannot be drawn for the rotational states as for the vibrational states. Figure 1 together with Fig. 2 permits one to visualize the connection of the reagent (b^*, E^*) pair with the product (v^*, R^*) pair. This is schematically sketched in Fig. 3, and a phase space "cell" is seen to be bordered by four curves, $v^* - 1/2$, $v^* + 1/2$, $R^* - dR^*/2$, and $R^* + dR^*/2$.

We define several quantities in advance (see Fig. 3). The limiting impact parameters, which correspond to the

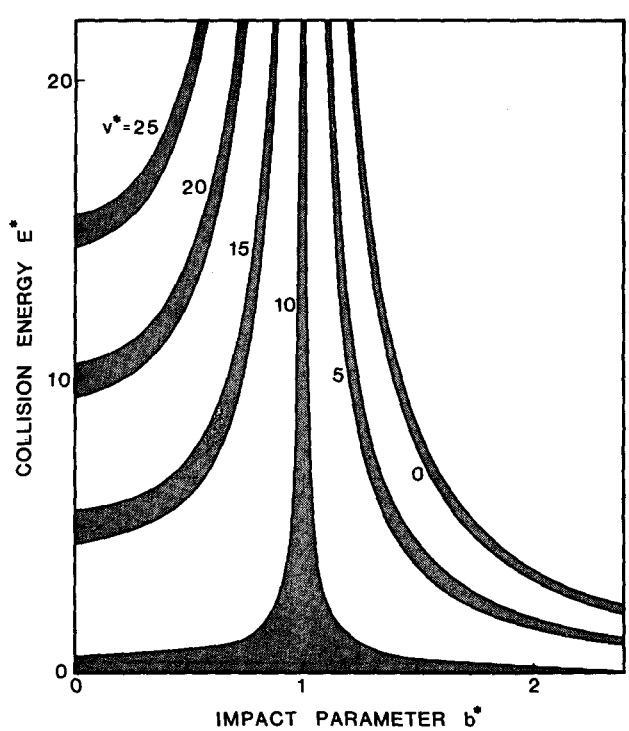

FIG. 1. Relation between (b^*, E^*) pair to the product vibrational level v^*. The value of A^* is set to 10. The region to the right of the $v^* = 0$ band is nonreactive due to insufficient energy.

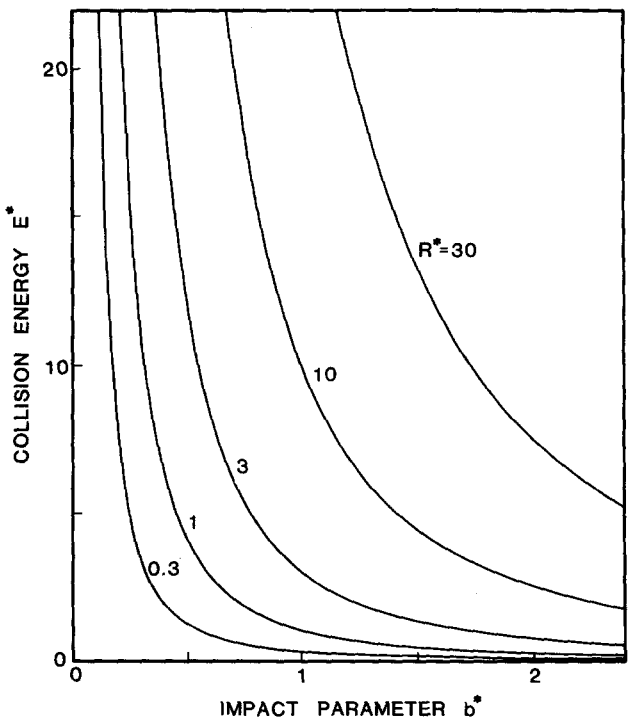

FIG. 2. Relation between the (b^*,E^*) pair to the product rotational energy R^*. When $R^* = 0$, the line falls onto the y and x axes. Note that most of the $R^* = 30$ contour belongs to the nonreactive phase space (see Fig. 1).

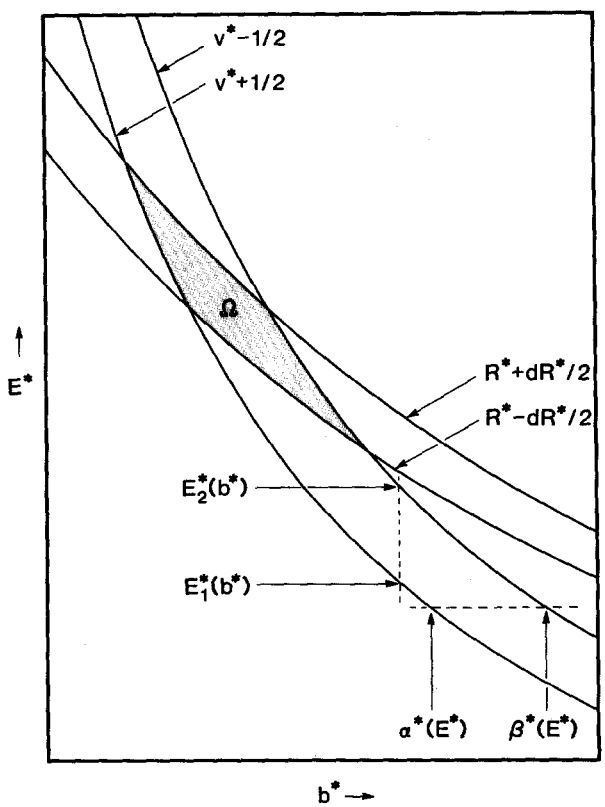

FIG. 3. Schematic diagram displaying the phase space cell (hatched area) which leads to the product (v^*,R^*) state. The width of the rotational state is exaggerated. The locations of $\alpha^*(E^*)$, $\beta^*(E^*)$, $E_1^*(b^*)$, and $E_2^*(b^*)$ are also shown.

vibrational energies $v^* + 1/2$ and $v^* - 1/2$ at a given collision energy E^*, are represented by $\alpha(E^*)$ and $\beta(E^*)$, respectively. Expressions for $\alpha(E^*)$ and $\beta(E^*)$ are obtained from Eq. (10):

$$\alpha(E^*) = [1 - (v^* + \tfrac{1}{2} - A^*)/E^*]^{1/2},$$
$$\beta(E^*) = [1 - (v^* - \tfrac{1}{2} - A^*)/E^*]^{1/2}, \qquad (13)$$

if the reaction is energetically permissible, and a value of zero is taken if $\alpha(E^*)$ or $\beta(E^*)$ becomes imaginary (i.e., the reaction is not allowed). The value of $b^*(E^*)$ for $v = 0$ is specially denoted by $\beta_{v=0}(E^*)$, which is the largest energetically permissible impact parameter at the collision energy E^*; if the impact parameter is greater than $\beta_{v=0}(E^*)$, then the reaction does not occur due to insufficient energy. In the same manner, we define the limiting collision energies, $E_1^*(b^*)$ and $E_2^*(b^*)$ $[E_2^*(b^*) > E_1^*(b^*)]$, which lead to the vibrational level v^* at a given impact parameter. The expressions for $E_1^*(b^*)$ and $E_2^*(b^*)$ are derived from Eq. (10) and are summarized in Table I.

With Eqs. (10) and (12), it is straightforward to calculate the probability to populate a single rovibronic state by finding the area of the cell corresponding to each (v^*,R^*) state weighted by the collision energy distribution, $f(E^*)$, and the reaction probability, $P(b^*,E^*)$. We thus define $P(v^*,R^*)dR^*$ as the probability[5] to populate a product in a vibrational level v^* with the rotational energy between $R^* - dR^*/2$ and $R^* + dR^*/2$:

$$P(v^*,R^*)dR^* = \frac{\int\int_\Omega f(E^*)P(b^*,E^*)b^*db^*dE^*}{\int_0^\infty \int_0^{\beta_{v=0}(E^*)} f(E^*)P(b^*,E^*)b^*db^*dE^*}. \qquad (14)$$

The integration limits are represented by Ω (see Fig. 3), and correspond to the cell which is associated with the (v^*,R^*) level. In many cases, a desired quantity can be calculated by the integration over the (b^*,E^*) phase space. However, the calculation of the product (v^*,R^*) state distribution can be simplified further by rewriting Eq. (14) as a double integral over v^* and R^* by a change of variables, i.e.,

TABLE I. Expressions for $E_1^*(b^*)$ and $E_2^*(b^*)$.

Condition	Expression
$v^* < A^*$, $b^* > 1$	$E_1^*(b^*) = (v^* + 1/2 - A^*)/(1 - b^{*2})$
	$E_2^*(b^*) = (v^* - 1/2 - A^*)/(1 - b^{*2})$
$v^* < A^*$, $b^* \leqslant 1$	$E_1^*(b^*)$ and $E_2^*(b^*) = 0$
$v^* = A^*$, $b^* < 1$	$E_1^*(b^*) = 0$
	$E_2^*(b^*) = (v^* + 1/2 - A^*)/(1 - b^{*2})$
$v^* = A^*$, $b^* = 1$	$E_1^*(b^*) = 0$
	$E_2^*(b^*) = \infty$
$v^* = A^*$, $b^* > 1$	$E_1^*(b^*) = 0$
	$E_2^*(b^*) = (v^* - 1/2 - A^*)/(1 - b^{*2})$
$v^* > A^*$, $b^* < 1$	$E_1^*(b^*) = (v^* - 1/2 - A^*)/(1 - b^{*2})$
	$E_2^*(b^*) = (v^* + 1/2 - A^*)/(1 - b^{*2})$
$v^* > A^*$, $b^* \geqslant 1$	$E_1^*(b^*)$ and $E_2^*(b^*) = 0$

$$P(v^*,R^*)dR^* = \frac{\int_{v^*-1/2}^{v^*+1/2}\left[\int_{R^*-dR^*/2}^{R^*+dR^*/2} f(E^*)P(b^*,E^*)b^*|J|^{-1}dR^*\right]dv^*}{\int_{-1/2}^{\infty}\left[\int_0^{\infty} f(E^*)P(b^*,E^*)b^*|J|^{-1}dR^*\right]dv^*}, \tag{15}$$

where

$$J = \begin{vmatrix} \frac{\partial v^*}{\partial b^*} & \frac{\partial R^*}{\partial b^*} \\ \frac{\partial v^*}{\partial E^*} & \frac{\partial R^*}{\partial E^*} \end{vmatrix} \tag{16}$$

is the Jacobian of the transformation. By using Eqs. (10) and (12), it is readily shown that

$$J = -2b^*E^*. \tag{17}$$

Therefore, Eq. (14) becomes

$$P(v^*,R^*)dR^* = \frac{\int_{v^*-1/2}^{v^*+1/2}\left[\int_{R^*-dR^*/2}^{R^*+dR^*/2} f(E^*)P(b^*,E^*)E^{*-1}dR^*\right]dv^*}{\int_{-1/2}^{\infty}\left[\int_0^{\infty} f(E^*)P(b^*,E^*)E^{*-1}dR^*\right]dv^*} \tag{18}$$

and the variables b^* and E^* are to be replaced by $[R^*/(v^*+R^*-A^*)]^{1/2}$ and $v^*+R^*-A^*$, respectively [see Eqs. (10) and (12)].

In the following, the reaction probability $P(b^*,E^*)$ is assumed to have the form

$$P(b^*,E^*) = p, \tag{19a}$$

when $b^* \leqslant \min[b^*_{\max}, \beta_{v=0}(E^*)]$, and

$$P(b^*,E^*) = 0, \tag{19b}$$

when $b^* > \min[b^*_{\max}, \beta_{v=0}(E^*)]$ and $0 < p \leqslant 1$. The value of p does not explicitly change the results of the following calculations, but is included to imply that the reaction probability need not be unity. The reaction probability $P(b^*,E^*)$ is nonzero for b^* less than some critical impact parameter, which is determined either by an energetic requirement [by $\beta_{v=0}(E^*)$] or some dynamic property for the reaction system (by $b^*_{\max}$). This quantity $b^*_{\max}$ is introduced to represent, for example, the crossing radius for ionic and covalent surfaces or the location of the centrifugal barrier in the entrance channel. In this model, $b^*_{\max}$ is considered to be an adjustable parameter, and the value is assumed to be independent of the collision energy.

The collision energy distribution is arbitrarily described by

$$f(E^*) = (E^*-E_0^*)\exp[-(E^*-E_0^*)/s^*] \quad \text{for } E^* \geqslant E_0^*,$$
$$= 0 \quad \text{for } E^* < E_0^*, \tag{20}$$

with two parameters, s^* being the width of the distribution (i.e, temperature) and E_0^* being the shift of the energy which, for example, pertains to a supersonic expansion. For this form of the collision energy distribution, the most probable collision energy is $E^* = s^* + E_0^*$, while the average collision energy $\langle E^* \rangle = 2s^* + E_0^*$, where $\langle E^* \rangle$ is defined as

$$\langle E^* \rangle = \frac{\int_0^{\infty} E^* f(E^*)dE^*}{\int_0^{\infty} f(E^*)dE^*}. \tag{21}$$

A translational energy barrier can also be included in the form of the collision energy distribution, but was not included in the following computations. Other forms of the collision energy distributions are discussed in the Appendix.

III. CALCULATION OF EXPERIMENTAL OBSERVABLES

A. Product vibrational distribution

It is possible to compute the vibrational populations by carrying out the summation over all rotation energies which can be done using Eq. (14):

$$P(v^*) = \int_0^{\infty} P(v^*,R^*)dR^* = \frac{\int_0^{\infty} f(E^*)\left[\int_{\alpha(E^*)}^{\beta(E^*)} P(b^*,E^*)b^*db^*\right]dE^*}{\int_0^{\infty} f(E^*)\left[\int_0^{\beta_{v=0}(E^*)} P(b^*,E^*)b^*db^*\right]dE^*}, \tag{22}$$

where $\alpha(E^*)$ and $\beta(E^*)$ are defined in Eq. (13) and

$$\sum_{v^*=0}^{\infty} P(v^*) = 1. \tag{23}$$

Since there are two intrinsic parameters, $b^*_{\max}$ and A^*, and two experimental parameters, E_0^* and s^*, we shall examine the effect of these parameters on the product vibrational distributions. Figure 4 displays the vibrational distributions for different $b^*_{\max}$ values. The populations of lower vibrational levels vary with $b^*_{\max}$, but those of higher levels do not change. When the values of A^* are varied, the peak of the vibrational population distribution shifts and coincides with the value of A^* (Fig. 5).

The effect of s^* is shown in Fig. 6. Again the peak of the distribution is determined by the value of A^*, and the form of the collision energy distribution affects only the width of the vibrational populations. In Fig. 7, the width of the collision energy distribution is kept constant, but the most probable

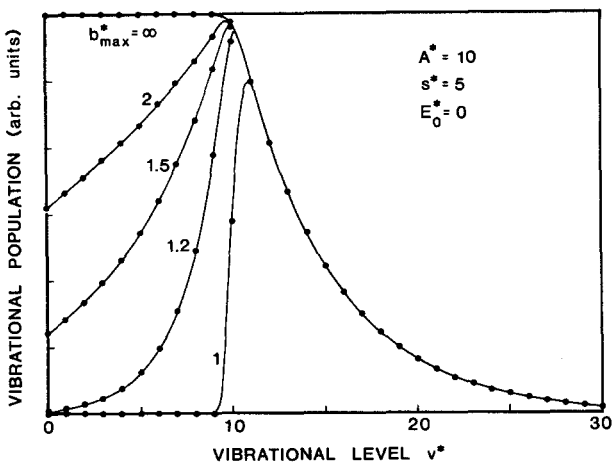

FIG. 4. Product vibrational populations for different values of b^*_{max}. The populations are made to join smoothly with the $b^*_{max} = \infty$ populations.

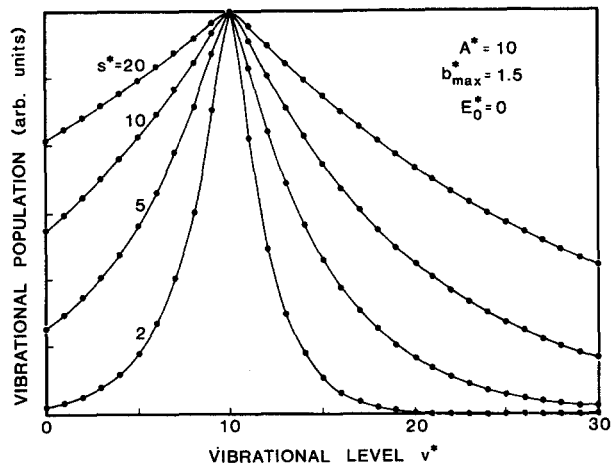

FIG. 6. Product vibrational populations for different values of s^*. The populations are normalized to unity.

collision energy is changed. As the collision energy distributions move to higher energy, the vibrational distributions become wider. However, the peak of the vibrational distribution remains at $v^* = A^*$.

B. The specific opacity function

Figure 8 displays the specific opacity function normalized to unity for several product vibrational channels when $A^* = 10$. The specific opacity function, $P_{v^*}(b^*)$, is calculated as

$$P_{v^*}(b^*) = \int_{E_1^*(b^*)}^{E_2^*(b^*)} f(E^*)dE^* \Big/ \int_0^\infty f(E^*)dE^*, \quad (24)$$

where $E_1^*(b^*)$ and $E_2^*(b^*)$ are defined in Table I. As can be speculated from Fig. 1, when $v^* = A^*$, $P_{v^*}(b^*)$ is very narrow and peaks at $b^* = 1$. When $v^* < A^*$, $P_{v^*}(b^*)$ is broad and extends past $b^* = 1$; when $v^* > A^*$, $P_{v^*}(b^*)$ is broad and does not extend past $b^* = 1$.

C. Product rotational energy distribution and average rotational energy

The product rotatational energy distributions for several vibrational levels are shown in Fig. 9 for $A^* = 10$, and Fig. 10 displays the average rotational energies, $\langle R^*(v^*)\rangle$, which are defined as

$$\langle R^*(v^*)\rangle = \int_0^\infty R^* P(v^*,R^*)dR^* \Big/ \int_0^\infty P(v^*,R^*)dR^*. \quad (25)$$

This can be rewritten by using Eq. (14) as

$$\langle R^*(v^*)\rangle = \frac{\int_0^\infty f(E^*)\left[\int_{\alpha(E^*)}^{\beta(E^*)} R^* P(b^*,E^*)b^* db^*\right]dE^*}{\int_0^\infty f(E^*)\left[\int_{\alpha(E^*)}^{\beta(E^*)} P(b^*,E^*)b^* db^*\right]dE^*}. \quad (26)$$

As seen in Fig. 9, the rotational energy distribution appears identical for $v^* \geqslant A^*$, resulting in constant rotational energies for those vibrational levels. This result is caused by our choice of the collision energy distribution: The numerator of the Eq. (18) contains a function $f(E^*)P(b^*,E)b^*|J|^{-1}$, which is $\exp[-(E^* - E_0^*)/s^*]$. Consequently when $E_0^* = 0$, $P(v^*,R^*)dR^*$ becomes

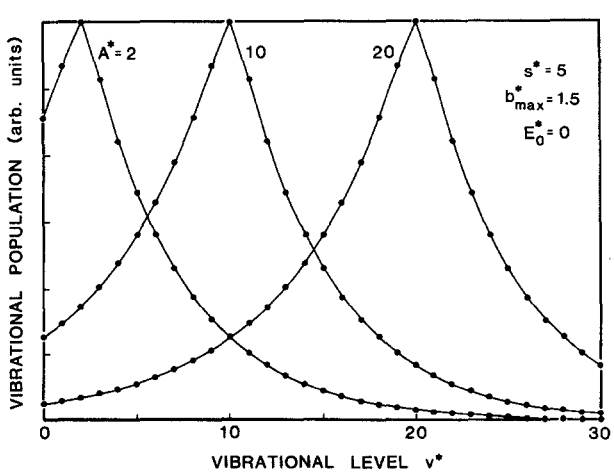

FIG. 5. Product vibrational populations for different values of A^*. The populations are normalized to unity.

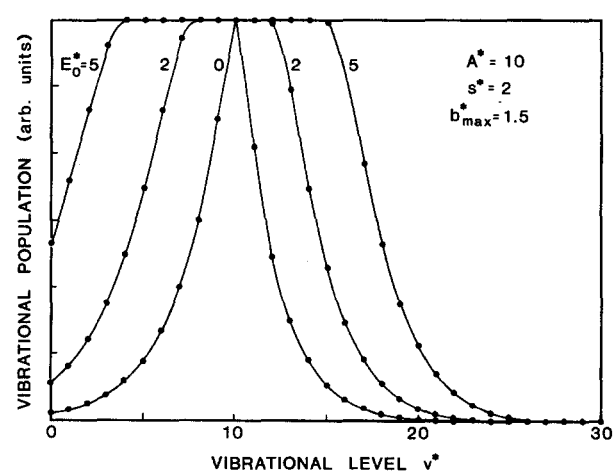

FIG. 7. Product vibrational populations for different values of E_0^*. The populations are normalized to unity.

$$P(v^*,R^*)dR^* \propto \int_{v^*-1/2}^{v^*+1/2}\left[\int_{R^*-dR^*/2}^{R^*+dR^*/2}\exp[-(v^*+R^*-A^*)/s^*]dR^*\right]dv^*$$
$$\approx dR^*\int_{v^*-1/2}^{v^*+1/2}\exp[-(v^*+R^*-A^*)/s^*]dv^*$$
$$= dR^*\exp[-(v^*+R^*-A^*)/s^*] \quad \text{for } R^* \geqslant A^*-v^*$$
$$= 0 \quad \text{for } R^* < A^*-v^*, \tag{27}$$

using a box integral. Thus the rotational distributions become an exponential of R^* for $v^* > A^*$, and they appear identical. However, the general trend of the average rotational energy, namely, that it decreases linearly for v^* up to $v^* = A^*$ and changes its slope more slowly for $v^* > A^*$ is independent of the form of the collision energy distributions (see the Appendix).

IV. DISCUSSION

A. Predictions of the CPR model

It was demonstrated in the last section that once the CPR approximation is adopted, the experimental observables can be computed in a straightforward manner. This is a direct consequence of the kinematic constraint for the reactive system to which the CPR model is applied: the rotational motion and the angular momentum are kinematically constrained. Consequently, once the value of the product recoil energy is fixed, the product vibrational energy is uniquely determined. In other words, the vibrational motion of the product is kinematically constrained as well as the rotation in the framework of the CPR model. This idea can be contrasted with the more general view that the product vibrational distribution is a dynamical property of the reaction and is a direct probe of the potential energy surface for the reaction system.

The information on the dynamics of the kinematically constrained reaction is contained in the values of A^* and b^*_{max} in the CPR model. The former reflects the value of the product recoil energy and the latter determines the largest impact parameter. These dynamical properties can be studied by measuring the product vibrational distribution at different collision energies, or by measuring the product rotational distributions preferably at low vibrational levels to probe the largest impact parameter.

The vibrational distribution calculated from the CPR model is generally bell-shaped (Figs. 4–7) and the width varies as the collision energy distribution changes. The most populated vibrational level has the energy equal to the value of A^*, which is essentially the exoergicity minus the recoil energy. This results from the fact that the vibrational level $v^* = A^*$ can be populated in two cases, when $b^* = 1$ and when $E^* = 0$. Because of this, the phase space for the $v^* = A^*$ level is the largest, causing the most populated level to be at $v^* = A^*$.

It may be informative to investigate the behavior of the vibrational distribution by evaluating the integral in the numerator of Eq. (22). We assume $b^*_{max} = \infty$. Using Eq. (19), the first integral can be shown to be $[\beta^2(E^*) - \alpha^2(E^*)]/2$, which becomes $(2E^*)^{-1}$ using Eq. (13), provided that the vibrational level v^* is accessible at the collision energy E^*. Therefore, the vibrational population is approximately expressed as

$$P(v^*) \propto \int_x^\infty f(E^*)E^{*-1}dE^*, \tag{28}$$

where x is zero for v^* less than A^*, and $x = v^* - A^*$ for $v^* > A^*$. Consequently, the populations for $v^* < A^*$ are

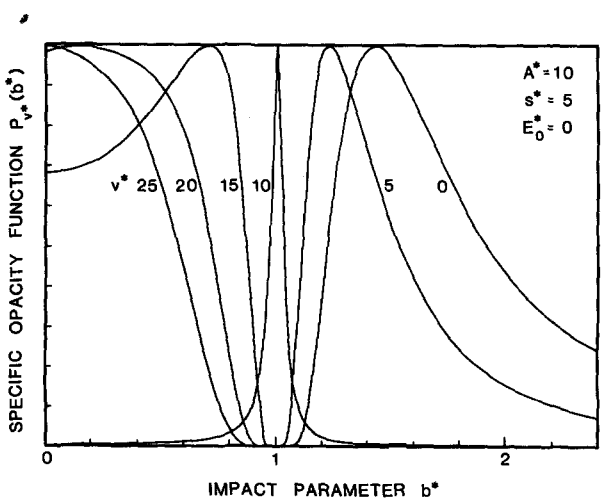

FIG. 8. Specific opacity function for several product vibrational levels. Each function is normalized to unity at the peak. The value of b^*_{max} is taken to be infinite, and if $b^*_{max} \neq \infty$, the specific opacity functions vanish for $b^* > b^*_{max}$. For the corresponding vibrational distribution, see Fig. 4.

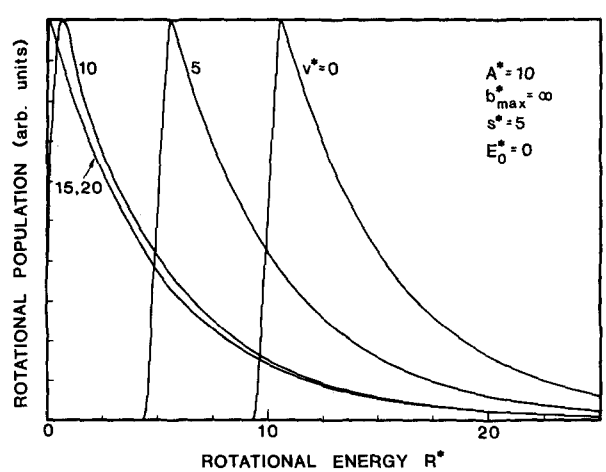

FIG. 9. Product rotational energy distributions in several vibrational levels. The distributions for v^* higher than $v^* = 10$ appear identical. For the corresponding vibrational distribution, see Fig. 4.

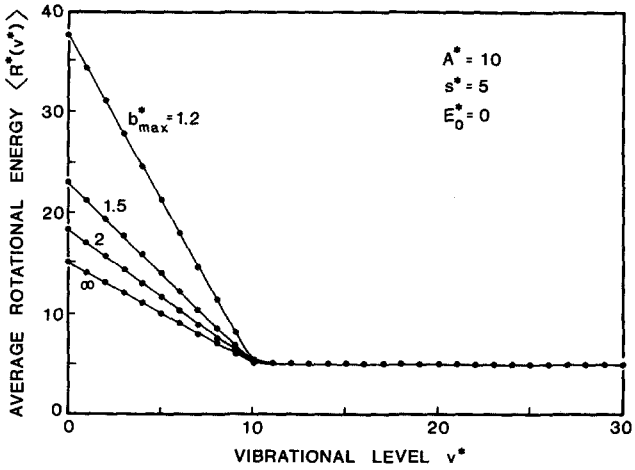

FIG. 10. Average product rotational energies as a function of b^*_{max}. The energies decrease linearly for $v^* < 10$, and are constant for $v^* > 10$.

equal when $b^*_{max} = \infty$ (see Fig. 5), and the populations slowly decrease for increasing v^* since the available range of collision energy becomes smaller. When $b^*_{max} \neq \infty$, the phase space at the large impact parameter becomes nonreactive, reducing the populations at lower vibrational levels more effectively. It should be noted that the vibrational population will appear to be a step function if the collision energy distribution is very narrow.

There exists in the CPR model a strong correlation between the impact parameter and the product vibrational level, which arises from an energy partitioning between the rotational and the vibrational states. Therefore, in head-on collisions (i.e., $b^* = 0$), all available energy must remain in vibration, leading to higher vibrational states, and if the impact parameter is large, energy goes into the rotational motion and the vibrational energy must be small. Consequently, the CPR model predicts that *small values of the impact parameter produce high vibrational excitation with low rotational excitation while large values produce low vibrational excitation with high rotational excitation.*

The specific opacity function for the most populated vibrational level, $P_{v^*=A^*}(b^*)$, is sharply peaked at the impact parameter equal to the equilibrium internuclear distance of the product diatomic molecule. Why is this the case? From Eq. (10), we find that b^* must be equal to 1 in order to produce $v^* = A^*$, i.e., $b = r_e$. Therefore the specific opacity function must be a δ function peaking at $b^* = 1$, if the width of the vibrational energy is ignored.

The average rotational energy in each vibrational level decreases linearly at $v^* < A^*$, and then starts to vary more slowly. When $b^*_{max} = \infty$, the average rotational energy decreases by 1 for each vibrational level, since each vibrational level takes one unit of energy out of total available energy, subtracting one from the rotational energy. When $b^*_{max} < \infty$, the average rotational energy decreases more rapidly, for the phase space associated with smaller rotational excitation no longer leads to reaction. Thus, the rotational energy distributions lose their lower energy portions and the average rotational energy becomes greater. It might appear puzzling that the rotational distributions for $v^* > A^*$ are identical and the specific opacity functions are different, whereas the average rotational energies for $v^* > A^*$ are equal. This is because the collision energy distribution is different for each product vibrational level since, for the given vibrational level v^*, the collision energy E^* less than $v^* - A^*$ cannot lead to reaction (see Fig. 1). Thus if one tries to deduce the specific opacity function from the rotational distribution, the collision energy distribution must be corrected for this "vibrational endoergicity."

The vibrational endoergicity and the fact that more phase space is available for reaction with lower collision energy suggest that the average collision energy defined in Eq. (21) does not correctly represent the average value of the reactive collision energy distribution. Thus we obtain an inequality

$$\langle E^* \rangle + \Delta E^* \neq v^* + \langle R^*(v^*) \rangle + \langle T^{f*} \rangle , \qquad (29)$$

where the quantities in brackets represent average values. Note that the reaction exoergicity and the average product recoil energy are given in reduced quantities. This inequality appears counterintuitive, and extreme care should be taken in estimating the average product recoil energy from energy balance. The equality can be recovered if we replace $\langle E^* \rangle$ by the average collision energy leading to reaction in which a vibrational level v^* is formed. This quantity is denoted by $\langle E^*(v^*) \rangle$ and expressed as

$$\langle E^*(v^*) \rangle = \frac{\int_0^\infty E^* f(E^*) \left[\int_{\alpha(E^*)}^{\beta(E^*)} P(b^*, E^*) b^* db^* \right] dE^*}{\int_0^\infty f(E^*) \left[\int_{\alpha(E^*)}^{\beta(E^*)} P(b^*, E^*) b^* db^* \right] dE^*} . \qquad (30)$$

Then we write

$$\langle E^*(v^*) \rangle + \Delta E^* = v^* + \langle R^*(v^*) \rangle + \langle T^{f*} \rangle . \qquad (31)$$

It must be pointed out that the sum of $\langle E^*(v^*) \rangle$ over all product vibrational states is still different from $\langle E^* \rangle$ since the lower collision energies are more heavily weighted.

So far, we confined our discussions to a heavy + heavy–light → heavy–heavy + light reaction (1), in which a particular mass combination constrained the reagent orbital angular momentum to appear as a product rotational angular momentum. It can be realized immediately that the equality, $|\mathbf{J}| = |\mathbf{L}|$, can be obtained whenever the product orbital angular momentum is negligible. This is true when either the impact parameter for the product repulsion or the product recoil energy is nearly zero. For these two cases, we may apply the CPR model to the reaction even if the system is not kinematically constrained (but the two reduced masses, μ and μ', should be carefully distinguished in these cases).

B. Comparison with experimental results

There have been numerous studies on kinematically constrained reactions. We may make comparisons of the predictions of the CPR model with some selected experimental results. In the following, we examine the validity of the CPR approximation semiquantitatively since it is beyond the scope of this article to use the collision energy dis-

tributions applicable in each experiment. It must be remembered that, in addition to the CPR approximation, we assumed the reaction probability, $P(b^*,E^*)$, is independent of the impact parameter and the collision energy [Eq. (19)].

1. Ba+HF→BaF+H

Gupta, Perry, and Zare[6] studied the Ba + HF → BaF + H reaction under crossed-beam conditions, and measured the vibrational distributions and the average rotational energy in each product vibrational level for different collision energy distributions. The reaction exoergicity is 4.4 kcal/mol and the vibrational frequency of the ground state vibration is 1.34 kcal/mol, so the value of A^* should be less than 3.3. The vibrational population in general appear bell-shaped with the maximum lying at $v = 1$ when $\langle E_{\rm col}\rangle = 1.6$ kcal/mol, and at $v = 2$ when $\langle E_{\rm col}\rangle = 6.5$ kcal/mol, suggesting that the value of A^* is approximately 2 and that the product recoil energy is about 1.7 kcal/mol. When the average collision energy is 13.5 kcal/mol, the product vibrational population does not appear bell-shaped, but linearly decreases for increasing v. The average rotational energy in a given vibrational level decreases slowly for increasing v with a slight change in slope at $v\approx 2$. The experimental results at lower collision energies agree fairly well with the predictions of the CPR model. But the vibrational distribution for $\langle E_{\rm col}\rangle = 13.5$ kcal/mol is different from the expected bell-shaped distribution and this may indicate the CPR approximation may fail at higher collision energies.

2. Ba+CH_3Br→BaBr→CH_3

Munakata, Matsumi, and Kasuya[7] studied the energy disposal in the reaction Ba + CH_3Br → BaBr + CH_3 as a function of collision energy. However, the CPR model is not readily applicable to this system due to two reasons. First, the kinematic constraint is not so favorable as in the previous experiment, since the leaving CH_3 group may not be sufficiently light. Second, we must assume that the CH_3 group carries the same amount of internal energy independent of the impact parameter and the collision energy as well as the product recoil energy. We must, therefore, apply the CPR model to this system with reservations.

This reaction is exoergic with $\Delta E = 16.7$ kcal/mol, and the vibrational frequency of the ground state equals 192.47 cm^{-1}. For the range of the collision energies studied (2.9 to 4.9 kcal/mol), the product vibrational distributions appear to be bell-shaped with the maximum lying between $v = 12$ when $\langle E_{\rm col}\rangle = 2.9$ kcal/mol and $v = 10$ when $\langle E_{\rm col}\rangle = 4.1$ kcal/mol. The exception is the vibrational population when $\langle E_{\rm col}\rangle = 4.9$ kcal/mol, in which case the vibrational population is nearly flat for $v < 10$ and then decreases for increasing v. The average rotational energy in each vibrational level shows a distinct feature; $\langle E_{\rm rot}(v)\rangle$ decreases linearly between $v = 0$ and $v\sim 10$, and then $\langle E_{\rm rot}(v)\rangle$ starts to vary very slowly. These trends are in good agreement with the predictions of the CPR model, and we roughly estimate the value of A should be 5.5 kcal/mol and the recoil energy is around 11 kcal/mol, and the $b^*_{\rm max}$ is about 1.5.

3. Ba+CF_3I→BaI+CF_3

The product state distribution of BaI produced by the Ba + CF_3I reaction has been studied by Johnson, Allison, and Zare.[8] This reaction is even less kinematically constrained than the Ba + CF_3Br system discussed above. However, the vibrational distribution is bell-shaped with the peak lying at $v\approx 50$. In addition, they concluded that increasing vibrational excitation of the product is correlated with decreasing rotational excitation. This suggests that there exists energy partitioning between vibration and rotation of the product, and this idea is consistent with the CPR prediction. From the availability of the energy they speculated that the CF_3 product has little internal energy, and this may be the reason why the predictions of the CPR model are in agreement with the experimental results.

4. Ba+HI→BaI+H

The specific opacity function was deduced by Noda *et al.*[9] from the rotational distribution of the Ba + HI → BaI + H reaction for the $v = 8$ product BaI vibrational level. Unfortunately the exoergicity of the reaction, the height of the translational energy barrier, and the velocity dependence of the reaction probability are not precisely known. Consequently the specific opacity function could not be uniquely determined in this study. When the reaction is assumed to proceed with equal probability for any translational energy, the specific opacity function, $P_{v=8}(b)$, peaks sharply at $b = 2.6$ Å with the width of 1.0 Å (FWHM). The vibrational distribution is bell-shaped with the maximum lying at $v = 10\sim 12$.[10]

By considering the predictions of the CPR model, we estimate the value of A is about 3.4 kcal/mol from the vibrational energy of the $v = 10$ level, which places a lower limit for the dissociation energy of the BaI molecule at 74.0 kcal/mol. This might be compared to the upper limit of 78 kcal/mol determined by Johnson, Allison, and Zare.[8] The CPR model is able to predict with success the shape of the specific opacity function for a product vibrational level close to the maximum in the vibrational distribution. However, closer inspection reveals some discrepancies: Since the BaI $v = 8$ level lies below the most populated vibrational level, the specific opacity function predicted by the CPR model should extend beyond $b = r_e$. The equilibrium internuclear distance of BaI is reported to be 3.0. Å.[11] Therefore, the predicted specific opacity function has the maximum at the impact parameter which is slightly too large.

C. Beyond the CPR approximation

The constant product recoil approximation is so simple that it serves as a convenient test bed for comparison with experimental studies of kinematically constrained bimolecular reactions. Surely this is a virtue. However, simplicity may also be its downfall. We expect that product recoil energy will be constant in general over a limited range of collision energies for direct kinematically constrained reactions. Connor *et al.*[12] examined the F + HF→F_2 + H reaction using

quasiclassical trajectories. Their results for this kinematically constrained system show that the fraction of available product energy in translation $\langle f_{Tf} \rangle$ is nearly a constant fraction of the initial collision energy. This indicates that the CPR approach will fail in some cases. In this section, we present possible extensions of the CPR model and investigate their applicability.

An obvious and more flexible approach is to assume a power series expansion for the dependence of the product recoil energy on the collision energy:

$$T^f = \sum_j k_j (T^i)^j / j! \tag{32}$$

which still assumes that T^f is the same for all impact parameters that lead to reaction. It is interesting to keep the first two terms of Eq. (32):

$$T^f = k_0 + k_1 T^i , \tag{33}$$

i.e., T^f has a linear dependence on T^i. We refer to this approximation as the linearly varying product recoil (LVPR) model. With this modification, Eq. (10) becomes

$$v^* = (1 - k_1 - b^{*2}) E^* + A_0^* , \tag{33}$$

where using Eq. (11c),

$$A_0^* = [\Delta E - k_0 + E(\mathrm{A}) + E(\mathrm{BC}) - E(\mathrm{C})]/\omega_e . \tag{34}$$

Thus the expression for v^* has the same mathematical form as Eq. (10) [and would reduce to Eq. (10) if $k_1 = 0$].

This expression can be further simplified by dividing both sides by $1 - k_1$, and we obtain

$$v^\circ = (1 - b^{\circ 2}) E^\circ (1 - k_1) + A^\circ , \tag{35}$$

where

$$v^\circ = v^*/(1 - k_1) , \tag{36a}$$

$$b^\circ = b^*/(1 - k_1)^{1/2} , \tag{36b}$$

$$E^\circ = E^*/(1 - k_1) , \tag{36c}$$

and

$$A^\circ = A_0^*/(1 - k_1) . \tag{36d}$$

Note that Eq. (35) has the same form as Eq. (10), if the collision energy is multiplied by $1 - k_1$. Thus the predictions of the CPR model can be applied to the LVPR model without detailed calculations! Specifically, (1) the product vibrational distribution is bell-shaped, and the peak of the distribution is located at $v^* = A^*$ (i.e., $v^\circ = A^\circ$), (2) reactions with small impact parameters lead to products in high vibrational states with low rotational excitation, (3) the specific opacity function for $v^* = A_0^*$ peaks at $b^* = (1 - k_1)^{1/2}$ (i.e., $b^\circ = 1$) instead of $b^* = 1$ in the CPR model, and (4) the product rotational distribution and the average rotational distribution in each vibrational level have the same trend as predicted by the CPR approximation.

Probably the most interesting difference between the predictions of the CPR and LVPR models is that the peak of the specific opacity function is shifted to smaller values in the LVPR model. For example, if $k_1 = 0.5$, the specific opacity function for $v^* = A^*$ peaks at $b^* = 0.87$. This may explain why the peak of the specific opacity function for the $\mathrm{Ba} + \mathrm{HI} \rightarrow \mathrm{BaI}(v = 8) + \mathrm{H}$ reaction lies at a smaller value than the equilibrium internuclear distance of BaI.

It is possible to include more terms in the expansion, Eq. (31), as well as the dependence of the product recoil energy on the impact parameter. The addition of these terms, unfortunately, cannot lead to simple expressions like Eq. (10) and (35), and computation must be carried out in each case. However, it must be stressed that *as long as the product recoil energy is expressed as a function of the impact parameter and/or collision energy, the vibrational motion of the product is uniquely defined and the product energy partitioning can be discussed in terms of the dynamical and kinematic constraints of the reaction.*

As a last remark, we consider the case where the product recoil energy distribution is determined by some probability distribution. For example, the DIPR-DIP model suggests that the product recoil energy distribution becomes a Gaussian reflecting the ground state vibrational wavefunction of the AB reactant.[13] Nevertheless the CPR or LVPR models can be applied by carrying out the CPR computations first with several values of A^*, and then averaging the results over A^* weighted by their probabilities. This process is quite general since the CPR and LVPR models are based on energy conservation, which is always correct.

ACKNOWLEDGMENTS

We are grateful to J. S. McKillop, W. E. Ernst, and M. A. Johnson for their useful comments and for fruitful discussions. This work was supported by the National Science Foundation under NSF CHE 85-05926.

APPENDIX: EFFECTS OF OTHER FORMS OF THE COLLISION ENERGY DISTRIBUTION

Throughout the article, we used the collision energy distribution which is described by a simple function defined in Eq. (20). Here we consider two other forms of the collision energy distributions in order to test the conclusions stated in the article.

The first function is a Gaussian-type collision energy distribution, which is defined as

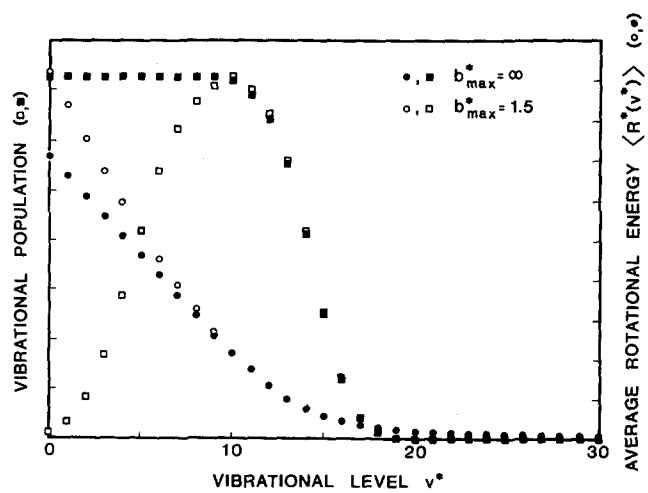

FIG. 11. Average product rotational energy (circles) and product vibrational population (squares) for the collision energy distribution described by Eq. (A1). The maximum impact parameter, b^*_{max}, is 1.5 (open symbols) and ∞ (solid symbols).

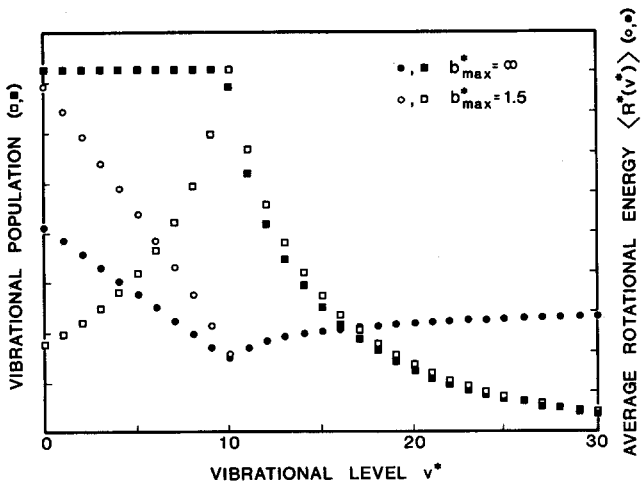

FIG. 12. Average product rotational energy (circles) and product vibrational population (squares) for the collision energy distribution described by Eq. (A2). The maximum impact parameter, b^*_{max}, is 1.5 (open symbols) and ∞ (solid symbols).

$$f(E^*) = \exp[-(E^* - E_0^*)^2/t^*], \quad \text{(A1)}$$

and the second function is defined as

$$f(E^*) = (E^* - E_0^*)^{-1/2} \exp[-(E^* - E_0^*)/u^*] \quad \text{for } E^* > E_0^*$$
$$= 0 \quad \text{for } E^* \leqslant E_0^*, \quad \text{(A2)}$$

where E_0^*, t^*, and u^* are adjustable parameters. For function (A1), the most probable collision energy is at $E^* = E_0^*$, and $\langle E^* \rangle \approx E_0^*$ with $E_0^* \gg t^*$. For function (A2), the most probable collision energy is at $E^* = E_0^*$, and $\langle E^* \rangle \approx u^*/2 + E_0^*$. We calculated the product vibrational distribution and the average rotational energy in each vibrational level when $b^*_{max} = 1.5$ and $b^*_{max} = \infty$. The results are displayed in Figs. 11 and 12 for functions (A1) and (A2), respectively. As can be seen from the figures, the exact calculations follow the predictions of the CPR model closely: The vibrational distributions are bell-shaped when $b^*_{max} \neq \infty$, and the average rotational energy decreases linearly for increasing v up to $v^* = A^*$, and then changes slowly its slope, i.e., decreases slowly for function (A1) and increases slightly for function (A2). Therefore, the predictions stated in this article may be compared with experimental observations. It must be noted, however, that the exact shapes of the calculated quantities depend on the form of the collision energy distribution applicable to each experiment, even though the general trends follow the CPR calculations presented.

[1] D. R. Herschbach, Adv. Chem. Phys. **10**, 233 (1966).
[2] R. B. Bernstein and B. E. Wilcomb, J. Chem. Phys. **67**, 5809 (1977).
[3] A. Siegel and A. Schultz, J. Chem. Phys. **76**, 4513 (1982).
[4] This unique mapping is a direct consequence of stepwise logic; the (b, v_{rel}) pair determines J by Eq. (5), J determines E_{rot} by Eq. (4b), and E_{rot} in turn determines E_{vib} by energy balance.
[5] Since the vibrational energy has the width of one energy unit, the width of the vibrational energy does not appear in the definition of the probability.
[6] A. Gupta, D. S. Perry, and R. N. Zare, J. Chem. Phys. **72**, 6237 (1980); Also see A. Gupta, Ph.D. thesis, Stanford University (1980).
[7] T. Munakata, Y. Matsumi, and T. Kasuya, J. Chem. Phys. **79**, 1698 (1983).
[8] M. A. Johnson, J. Allison, and R. N. Zare, J. Chem. Phys. **85**, 5723 (1986).
[9] C. Noda, J. S. McKillop, M. A. Johnson, J. R. Waldeck, and R. N. Zare, J. Chem. Phys. **85**, 856 (1986).
[10] H. W. Cruse, P. J. Dagdigian, and R. N. Zare, Faraday Discuss. Chem. Soc. **55**, 277 (1973).
[11] M. A. Johnson, C. Noda, J. S. McKillop, and R. N. Zare, Can. J. Phys. **62**, 1467 (1984).
[12] J. N. L. Connor, A. Leganà, A. F. Turfa, and J. C. Whitehead, J. Chem. Phys. **75**, 3301 (1981).
[13] P. J. Kuntz, E. M. Nemeth, and J. C. Polanyi, J. Chem. Phys. **50**, 4607 (1969); P. J. Kuntz, M. H. Mok, and J. C. Polanyi, *ibid.* **50**, 4623 (1969); D. R. Herschbach, Faraday Discuss. Chem. Soc. **55**, 233 (1973).